Published in final edited form as:
Sci Signal. ; 4(164): ra15. doi:10.1126/scisignal.2001464.

LRP6 Mediates cAMP Generation by G Protein–Coupled Receptors Through Regulating the Membrane Targeting of $G\alpha_s$

Mei Wan[1,*], **Jun Li**[1,2], **Katie Herbst**[3], **Jin Zhang**[3], **Bing Yu**[1], **Xiangwei Wu**[1,2], **Tao Qiu**[1], **Weiqi Lei**[1], **Charlotta Lindvall**[4], **Bart O. Williams**[4], **Hairong Ma**[1], **Fengjie Zhang**[1,2], and **Xu Cao**[1,*]

[1]Department of Orthopaedic Surgery, Johns Hopkins University School of Medicine, Baltimore, MD 21205, USA.

[2]Shihezi Medical College, Shihezi University, Xinjiang 832002, China.

[3]Department of Pharmacology and Molecular Science, Johns Hopkins University School of Medicine, Baltimore, MD 21205, USA.

[4]Laboratory of Cell Signaling and Carcinogenesis, Van Andel Research Institute, Grand Rapids, MI 49503–2518, USA.

Abstract

Ligand binding to certain heterotrimeric guanine nucleotide–binding protein (G protein)–coupled receptors (GPCRs) stimulates the rapid synthesis of cyclic adenosine monophosphate (cAMP) through the G protein α_s subunit, which activates adenylyl cyclase (AC). We found that the transmembrane receptor low-density lipoprotein receptor–related protein 6 (LRP6), a co-receptor for Wnt proteins, bound to the $G\alpha_s\beta\gamma$ heterotrimer and that knockdown of LRP6 attenuated cAMP production by various GPCRs, including parathyroid hormone receptor 1 (PTH1R). Knockdown of LRP6 disrupted the localization of $G\alpha_s$ to the plasma membrane, which led to a decrease in the extent of coupling of $G\alpha_s$ to PTH1R and inhibited the production of cAMP and the activation of cAMP-dependent protein kinase (PKA) in response to PTH. PKA phosphorylated LRP6, which enhanced the binding of $G\alpha_s$ to LRP6, its localization to the plasma membrane, and the production of cAMP in response to PTH. Decreased PTH-dependent cAMP production was observed in single cells in which LRP6 was knocked down or mutated at the PKA site by monitoring the cAMP kinetics. Thus, we suggest that the binding of $G\alpha_s$ to LRP6 is required to establish a functional GPCR-$G\alpha_s$-AC signaling pathway for the production of cAMP, providing an additional regulatory component to the current GPCR-cAMP paradigm.

INTRODUCTION

Cyclic adenosine monophosphate (cAMP) acts as a second messenger in prokaryotes and eukaryotes. The concentration of cytosolic cAMP is increased by an order of magnitude within seconds of the activation of heterotrimeric guanine nucleotide–binding protein (G protein)–coupled receptors (GPCRs), which typically have seven plasma membrane–spanning domains (1–3). This large family of receptors mediates many critical signaling

[*]To whom correspondence should be addressed. mwan4@jhmi.edu (M.W.); xcao11@jhmi.edu (X.C.).

Author contributions: M.W. and X.C. designed the research; M.W., J.L., K.H., J.Z., B.Y., X.W., T.Q., W.L., C.L., H.M., and F.Z. performed the research; M.W., J.Z., B.O.W., and X.C. analyzed the data; J.Z. and B.O.W. provided critical discussion of the results and commentary on the manuscript; and M.W. and X.C. wrote the paper.

SUPPLEMENTARY MATERIALS
www.sciencesignaling.org/cgi/content/full/4/164/ra15/DC1

Competing interests: The authors declare that they have no competing interests.

events, including the signaling of parathyroid hormone (PTH) in bone and kidney (4–6), adrenaline in heart and muscle (7, 8), glucagon in liver and fat (9, 10), vasopressin in kidney (11, 12), adrenocorticotropic hormone in the adrenal cortex (13, 14), and luteinizing hormone in the ovary (15, 16). The rapid synthesis of cAMP is achieved by the transmembrane enzyme adenylyl cyclase (AC), which is activated directly by the α_s subunit of the G protein that is associated with the GPCR.

The currently accepted paradigm for the production of cAMP is that the inactive form of $G\alpha_s$ is bound to guanosine diphosphate (GDP) at its guanine nucleotide–binding pocket and that $G\alpha_s$-GDP combines with the $\beta\gamma$ subunits of the G protein to form a heterotrimer with an inactive configuration at the cell membrane (1–3). The heterotrimer is thought to be attached to the cell membrane by hydrophobic interactions through lipid modifications of the G proteins, such as palmitoylation of $G\alpha_s$ (17–19) and isoprenylation of $G\gamma$ (20, 21). The binding of ligand to a GPCR alters the conformation of the associated $G\alpha_s$, promoting the release of GDP and the binding of guanosine triphosphate (GTP), as well as the depalmitoylation and disassociation of $G\alpha_s$ from the $\beta\gamma$ dimer. $G\alpha_s$ then associates with and activates AC, which results in the synthesis of cAMP (22).

Low-density lipoprotein receptor–related protein 6 (LRP6) belongs to the low-density lipoprotein receptor (LDLR) family (23, 24) and is widely abundant in human and mouse tissues. LRP6 has a large extracellular domain that contains 1372 amino acid residues anchored to the plasma membrane through a transmembrane domain that is followed by a relatively short cytoplasmic domain of 207 amino acid residues. LRP6 was initially characterized as a co-receptor that stabilizes β-catenin in the Wnt signaling pathway (25, 26), and its signaling is regulated by a large number of extracellular proteins, including members of the Dickkopf (Dkk) family (23, 27, 28) and sclerostin (29–31). In the absence of Wnts, β-catenin is found in a large cytoplasmic complex that consists of other proteins that promote its inactivation by phosphorylation and proteasomal degradation. In the presence of Wnts, Frizzled proteins, which are receptors for Wnts and share the basic structural organization of GPCRs, form complexes with their co-receptor LRP6. Phosphorylation of LRP6 at PPPS/TP motifs is then triggered, which is followed by the recruitment of axin to the plasma membrane (23), leading to inhibition of the phosphorylation and degradation of β-catenin. Stabilized β-catenin protein accumulates in the nucleus and forms complexes with the T cell factor–lymphoid enhancer factor (TCF-LEF) family of DNA binding transcription factors to enhance the expression of target genes to regulate cellular activities.

GPCRs other than Frizzled proteins, such as prostaglandin F_2 receptor FP_B (32), M1 acetylcholine muscarinic receptor (33), lysophosphatidic acid receptors (34), the prostaglandin E_2 receptor EP2 (35), gonadotrophin-releasing hormone receptor (36), and PTH receptor 1 (PTH1R) (37), also activate β-catenin signaling. In particular, the direct association of the active form of $G\alpha_s$ with the scaffolding protein axin regulates EP2-induced β-catenin signaling (35). Free $G\beta\gamma$ recruits glycogen synthase kinase 3 (GSK-3) to the plasma membrane to phosphorylate LRP6 at its PPPS/TP site, providing further evidence for the direct involvement of G proteins in the GPCR-stimulated stabilization of β-catenin (38). LRP6 likely acts as a common receptor in different GPCR signaling pathways mediated by the activation of G proteins because LRP6 forms complexes with various GPCRs in response to ligand stimulation (37). Here, we examined whether LRP6 was involved in $G\alpha_s$-mediated cAMP signaling. We found that knockdown of LRP6 inhibited the production of cAMP in response to different GPCR ligands. Upon ligand stimulation, LRP6 was phosphorylated by cAMP-dependent protein kinase (PKA), leading to its association with the $G\alpha_s\beta\gamma$ heterotrimer, which then accumulated at the plasma membrane to enable its coupling with GPCRs to trigger cAMP production.

RESULTS

LRP6 is required for PTH-dependent generation of cAMP

To examine the role of LRP6 in PTH-dependent cAMP production, we used small interfering RNA (siRNA) to knock down LRP6 or LRP5 in UMR-106 rat osteosarcoma cells (Fig. 1A) and C2C12 pluripotent mouse osteoprogenitor cells (Fig. 1B). We then treated the cells with PTH(1–34), a C-terminal–truncated synthetic analog of PTH that has an anabolic effect on bone formation in humans (39). Knockdown of LRP6 inhibited the PTH (1–34)–stimulated accumulation of cAMP in both cell types, whereas knockdown of LRP5 did not affect cAMP production in C2C12 cells (Fig. 1B) and only moderately inhibited cAMP accumulation in response to PTH in UMR-106 cells (Fig. 1A). To further confirm the requirement for LRP6 in PTH-induced cAMP accumulation in primary osteoblasts, we isolated calvarial preosteoblasts from *lrp6*$^{flox/flox}$ or *lrp6*$^{flox/flox}$;*lrp5*$^{-/-}$ mice (40). The *lrp6* gene was deleted by adenovirus-mediated expression of the *Cre* recombinase gene. PTH-stimulated cAMP accumulation in primary preosteoblastswas inhibited by deletion of LRP6, but not of LRP5 (Fig. 1C).

Because PKA can be activated by cAMP that accumulates in response to the stimulation of G_s-coupled GPCRs, we examined the extent of PTH-stimulated phosphorylation of cAMP-responsive element (CRE)–binding protein (CREB), a transcription factor that is a direct downstream target of PKA (37, 38). Simultaneous knockdown of LRP5 and LRP6 inhibited the PTH-induced phosphorylation of CREB in UMR-106 cells (Fig. 1D). Phosphorylation of CREB was partially inhibited when LRP6 alone was knocked down, which suggested that LRP5 might also play a role in PTH-activated cAMP-PKA signaling specifically in UMR-106 cells. To assess whether knockdown of LRP6 affected the temporal dynamics of cAMP production, we monitored the kinetics of cAMP generation in live cellswith Epac (ICUE3), a fluorescence resonance energy transfer (FRET)–based biosensor of cAMP production (41–43). PTH(1–34) induced a rapid change in the ratio of cyan-to-yellow emissions (an indication of cAMP production) within 30 s, which reached a plateau within ~4 to 6 min, whereas we observed a slower response to forskolin (Fig. 1E), a direct activator of AC (44). Cells in which LRP6 was knocked down exhibited a minimum response to PTH, whereas cells in which LRP5 was knocked down had a slightly smaller response to PTH than that of the control cells (Fig. 1F). These results indicate that LRP6 is required for PTH-activated cAMP-PKA signaling and that LRP5 plays a relatively minor role in this pathway.

LRP6 is required for the generation of cAMP in response to different GPCR ligands

To determine whether LRP6 was also required for the generation of cAMP by other G_s-coupled GPCRs, we examined the effects of LRP6 knockdown on cAMP production in various cell types by different agonists, including by isoproterenol, a β-adrenergic receptor agonist, in C2C12 cells (Fig. 2A), by adenosine in human bronchial smooth muscle cells (Fig. 2B), by glucagon in human embryonic kidney (HEK) 293 cells (Fig. 2C), and by isoproterenol in primary mouse embryo fibroblasts (MEFs) (Fig. 2D). The generation of cAMP was reduced by knockdown of LRP6 in all of these models (Fig. 2, A to D). The effect of forskolin on the production of cAMP was also inhibited by knockdown of LRP6, but was much less affected than was isoproterenol (Fig. 2D). By monitoring cAMP kinetics in live cells, we showed that the knockdown of LRP6 consistently reduced the responses of these cells to isoproterenol, but only mildly reduced the response of the cells to forskolin (Fig. 2E), indicating that the inhibition of cAMP production that occurred through loss of LRP6 was not primarily through the suppression of AC activity. Together, these data suggest that LRP6 is required in the production of cAMP by $G\alpha_s$-coupled GPCRs.

PTH promotes the association of LRP6 and $G\alpha_s$

To determine the mechanisms by which LRP6 was involved in cAMP production induced by $G\alpha_s$-coupled receptors, we examined the interaction of LRP6 with $G\alpha_s$ in a pull-down assay. We incubated glutathione *S*-transferase (GST)–fused cytoplasmic domains of LRP6 or LRP5 with lysates of HEK 293 cells and found that the intracellular domains of both LRP6 and LRP5 bound to $G\alpha_s$ from the cell lysates (Fig. 3A). This was further confirmed in an immunoprecipitation experiment in which HEK 293 cells were transfected with plasmid encoding PTH1R to render them susceptible to stimulation with PTH, together with plasmid encoding hemagglutinin (HA)–tagged LRP5 or vesicular stomatitis virus G (VSVG)–tagged LRP6. Immunoprecipitation followed by Western blotting analysis revealed that $G\alpha_s$ formed complexes with both LRP5 (Fig. 3B) and LRP6 (Fig. 3C) in the absence of PTH, and that PTH enhanced the interaction between $G\alpha_s$ and LRP6 within 5 min of treatment and that this association was further enhanced 30 min after addition of the ligand (Fig. 3C). In contrast, PTH did not enhance the association of $G\alpha_s$ with LRP5 (Fig. 3B).

$G\alpha_s$ and $G\beta\gamma$ form a heterotrimer on the cell membrane with an inactive configuration. Once activated, $G\alpha_s$ is dissociated from $\beta\gamma$ dimer. We next performed immunoprecipitations to examine whether LRP6 interacted with the $G\alpha_s\beta\gamma$ heterotrimer or with the free active form of $G\alpha_s$, and we found that LRP6 interacted with both $G\alpha_s$ and $G\beta_1$ (Fig. 3D). The interaction of LRP6 with $G\alpha_s$ was blocked by AlF_4^-, a compound that directly activates G protein α subunits, which indicated that the active form of $G\alpha_s$ did not interact with LRP6. Moreover, AlF_4^- also blocked the interaction of LRP6 with $G\beta_1$. Thus, LRP6 formed a complex with the inactive configuration of the $G\alpha_s\beta\gamma$ heterotrimer, and the interaction of LRP6 with $G\beta\gamma$ was mediated by the binding of $G\alpha_s$ to LRP6. Because the $G\alpha_o$ and $G\alpha_i$ proteins are also involved in regulating AC activity, we examined whether LRP6 also formed a complex with these G proteins. We found that LRP6 interacted with $G\alpha_s$, but had either an undetectable or a weak interaction with $G\alpha_o$ and $G\alpha_{i2}$ (Fig. 3E), indicating that LRP6 specifically bound to $G\alpha_s$.

$G\alpha_s$ interacts with the β-catenin destruction complex by binding to the scaffolding protein axin (35). We examined whether axin was involved in the interaction between $G\alpha_s$ and LRP6, but found that knockdown of axin did not affect the PTH-induced interaction between LRP6 and $G\alpha_s$ (Fig. 3F). Axin binds to the active rather than the inactive form of $G\alpha_s$ (35); therefore, our finding suggests that inactive $G\alpha_s$ binds to LRP6 and that $G\alpha_s$ binds to axin once it is activated. LRP6 aggregates rapidly in response to Wnt3a signaling (45, 46). Because PTH induced the association of $G\alpha_s$ with LRP6, we reasoned that $G\alpha_s\beta\gamma$ might be associated with LRP6 that had aggregated in response to PTH. We performed sucrose density gradient centrifugation and found that LRP6 was detectable in the lower–molecular mass fractions of unstimulated UMR-106 cells (Fig. 4, fractions 8 to 12). LRP6 was redistributed into the heavier fractions of samples that had been treated with PTH for 5 min (Fig. 4, fractions 6 and 7), and this redistribution was lost 30 min after PTH treatment. We detected $G\alpha_s$, $G\beta_1$, and $G\gamma_2$ in these heavier fractions in response to PTH stimulation. We did not observe the redistribution of these subunits into the heavier fractions in cells in which LRP6 was knocked down by siRNA. These results support the concept that PTH stimulated an interaction between LRP6 and the $G\alpha_s\beta\gamma$ heterotrimer and further suggest that LRP6 promoted the redistribution and clustering of $G\alpha_s\beta\gamma$ at the cell membrane in response to PTH. The development of localized high concentrations of $G\alpha_s$ could act to enhance the coupling of PTH1Rs to G proteins and play a role in the rapid generation of cAMP that is typical of GPCR stimulation.

LRP6 regulates the localization of $G\alpha_s$ to the plasma membrane

It is well established that in the absence of GPCR stimulation, G protein α subunits are in a complex with the β and γ subunits and are associated with the plasma membrane (17–19). These associations are a prerequisite for the coupling of GPCRs with G proteins and the activation of G protein α subunits in response to agonists. Moreover, the localization of G proteins at the cytoplasmic face of the plasma membrane is essential for the coupling of GPCRs to AC. We therefore tested whether LRP6 regulated the localization of $G\alpha_s\beta\gamma$ to the plasma membrane. Both $G\alpha_s$ and $G\beta_1$ were primarily localized to the plasma membrane in control cells and LRP5-deficient cells stably expressing either green fluorescent protein (GFP)–tagged $G\alpha_s$ or GFP-tagged $G\beta_1$ (Fig. 5, A and B). A portion of $G\alpha_s$ and $G\beta_1$ was localized to the cytosol when LRP6 was knocked down (Fig. 5, A and B). To test the possibility that PTH1R might also undergo trafficking from the plasma membrane to the cytosol in the context of knockdown of LRP6, we performed immunofluorescence analysis of HEK 293 cells stably expressing cyan fluorescent protein (CFP)–tagged PTH1R. PTH1R localized primarily to the plasma membrane, and knockdown of LRP6 did not affect its localization (Fig. 5, A and B), indicating that the amount of $G\alpha_s\beta\gamma$ that resided at the plasma membrane and that colocalized with plasma membrane–bound PTH1R was largely reduced when LRP6 was absent.

To confirm this observation in vivo, we generated osteoblast-specific LRP6 knockout mice by crossing *lrp6*$^{flox/flox}$ mice with *OC-Cre* mice. Immunohistological analysis of bone sections revealed that $G\alpha_s$ was localized primarily at the plasma membrane of osteoblasts in wild-type mice, whereas $G\alpha_s$ was found largely in the cytosol of osteoblasts from LRP6 knockout mice (Fig. 5, C and D). Furthermore, we examined whether LRP6 was also involved in the coupling of PTH1R to $G\alpha_s$, because we previously demonstrated that PTH induces the formation of a complex between LRP6 and PTH1R (37). The formation of the PTH1R-$G\alpha_s$ complex could be estimated by immunoprecipitation of PTH1R from lysates of HEK 293 cells that were stably transfected with a plasmid encoding HA-tagged PTH1R followed by Western blotting analysis for $G\alpha_s$, or vice versa. We found that the amount of the PTH1R-$G\alpha_s$ complex was reduced in cells in which LRP6 was knocked down compared to that in control cells (Fig. 5, E and F), but that knockdown of LRP5 had no effect (Fig. 5E), suggesting that LRP6 played a role in the formation of this complex. Together, these results indicated that LRP6 regulated the localization to the plasma membrane of a $G\alpha_s$ complex to enable its coupling with GPCRs to trigger the production of cAMP.

PTH induces the phosphorylation of LRP6 at a PKA target site

Sequence analysis of the intracellular domain of LRP6 revealed several consensus phosphorylation sites for PKA (RR/K-S*/T*; R-X_2-S*/T*; and R-X-S*/T*) (Fig. 6A, upper panel) (47). We therefore examined whether PKA directly phosphorylated LRP6. In vitro kinase assays demonstrated that the intracellular domain of LRP6 (LRP6C) was phosphorylated by PKA (Fig. 6A, lower panel). In contrast, the intracellular domain of LRP5 was not phosphorylated, which, together with our observation that PTH did not induce the aggregation of LRP5 or promote its interaction with $G\alpha_s$, further suggests that LRP6 plays the predominant role in regulating PTH1R signaling and that phosphorylation of LRP6 by PKA in turn may affect cAMP-PKA signaling. To test this directly, we first used site-directed mutagenesis to modify the individual putative PKA phosphorylation sites in LRP6C. Only alteration of Thr^{1548} abolished the phosphorylation of LRP6C by PKA (Fig. 6B), and mass spectrometry analysis confirmed that Thr^{1548} was the PKA phosphorylation site in LRP6C (fig. S1). We then transfected HEK 293 cells with plasmid encoding the HA-tagged cytoplasmic domain of wild-type LRP6 or a HA-tagged cytoplasmic domain of LRP6 from which the PKA site was deleted (fig. S2), and we analyzed the interaction between $G\alpha_s$ and LRP6 by immunoprecipitation and Western blotting. Deletion of the PKA

phosphorylation site (in the mutants LRP6Δ108 or LRP6Δ78) from LRP6 reduced the extent of the interaction with $G\alpha_s$ compared to that between wild-type LRP6 and $G\alpha_s$, whereas the addition of this site (LRP6Δ58) rescued, at least partially, the interaction (fig. S2), which suggested that phosphorylation of the PKA site enhanced the binding of $G\alpha_s$ to LRP6. The reason the extent of binding of $G\alpha_s$ to the LRP6Δ58 mutant was less than that with wild-type LRP6 (fig. S2) may be because the basal extent of binding between $G\alpha_s$ and LRP6 in the absence of ligand or agonist was independent of the phosphorylation state of LRP6. Removal of 58 amino acid residues from the C terminus of LRP6 might change the conformation of the protein and affect the basal binding to $G\alpha_s$.

GSK-3 is a regulatory kinase that preferentially phosphorylates proteins that have been already phosphorylated at other sites (47). Examination of the amino acid sequence adjacent to Thr^{1548} in LRP6 revealed a GSK-3 consensus site (Ser^{1544}) (Fig. 6C, upper panel). In an in vitro kinase assay, we confirmed that pretreatment with recombinant PKA enhanced the phosphorylation of LRP6 by GSK-3 (Fig. 6C, lower panel). We generated two LRP6C mutants, $LRP6C^{mPKA}$ and $LRP6C^{mGSK3}$, in which the PKA phosphorylation site (Thr^{1548}) or the GSK-3 phosphorylation site (Ser^{1544}) was mutated, respectively. Both mutants abolished the phosphorylation of LRP6 by GSK-3 (Fig. 6D). Thus, these data suggest that LRP6 was sequentially phosphorylated by PKA and GSK-3 at Thr^{1548} and Ser^{1544}.

Phosphorylation of LRP6 by PKA promotes its binding to $G\alpha_s$

We then examined the role of the PKA site of LRP6 in PTH signaling. Our earlier data provided the framework for further analysis of the effects of the PKA-mediated phosphorylation of LRP6 on the binding of $G\alpha_s$ to LRP6 and on its subcellular location, as well as its role in PTH-induced cAMP production. Sequential phosphorylation of LRP6 by PKA and GSK-3 stimulated the binding of $G\alpha_s$ to LRP6C, and mutation of the PKA site abolished the enhanced binding (Fig. 7, A and B). Moreover, PTH failed to stimulate the association of $G\alpha_s$ with a mutant LRP6 that was missing the PKA phosphorylation site ($LRP6^{mPKA}$) (Fig. 7C). To test whether the phosphorylation of LRP6 by PKA or GSK-3 regulated the subcellular localization of $G\alpha_s$, we transfected a stable cell line containing GFP-$G\alpha_s$ with plasmid encoding wild-type LRP6 or LRP6 mutants in which the mutation was at either the PKA ($LRP6^{mPKA}$) or the GSK-3β ($LRP6^{mGSK3}$) phosphorylation site. $G\alpha_s$ was primarily localized to the cell membrane in cells transfected with empty vector or plasmid encoding wild-type LRP6, but a portion of total $G\alpha_s$ was translocated to the cytosol in cells that expressed either $LRP6^{mPKA}$ or $LRP6^{mGSK3}$ (Fig. 7, D and E). As a result, isoproterenol-stimulated cAMP production was reduced in cells expressing either mutant compared to that in cells expressing wild-type LRP6 (Fig. 7F). To further examine the role of phosphorylation of LRP6 by PKA in the dynamics of cAMP production, we monitored cAMP kinetics in live cells. The production rate of cAMP at 2 min after isoproterenol stimulation was similar in cells that contained either wild-type LRP6 or $LRP6^{mPKA}$ (Fig. 7G). There was a much smaller response in cells expressing $LRP6^{mPKA}$ compared to that in cells expressing wild-type LRP6 at ~2 to 8 min after isoproterenol stimulation. Together, these results support the idea that phosphorylation of LRP6 at the PKA site enhances the binding of $G\alpha_s$ to LRP6 and accelerates the localization of $G\alpha_s$ to the plasma membrane to enable rapid signal amplification.

DISCUSSION

Although studies have shown that LRP6 is involved in the stabilization of β-catenin in response to GPCR stimulation, how LRP6 integrates the signaling of G proteins and β-catenin remains poorly understood. We propose a mechanism for the role of LRP6 in $G\alpha_s$-coupled, GPCR-stimulated production of cAMP in which LRP6 binds to the $G\alpha_s\beta\gamma$ heterotrimer and the ligands of GPCRs, such as PTH, promote this binding. The interaction

between LRP6 and $G\alpha_s\beta\gamma$ induced by PTH would cause the local accumulation of $G\alpha_s\beta\gamma$ at the plasma membrane to set up a functional GPCR-$G\alpha_s$-AC complex for the rapid production of cAMP and subsequent PKA activation. Activated PKAwould in turn phosphorylate LRP6 at its cytoplasmic domain and enhance its association with $G\alpha_s$ and the accumulation of $G\alpha_s\beta\gamma$ to amplify the signal (Fig. 8). Thus, the association of $G\alpha_s$ with LRP6 adds another dimension to the regulation of GPCR-mediated cAMP production.

The model that we propose also provides a better understanding of the roles of LRP6 in GPCR-dependent stimulation of two distinct signaling pathways, that is, β-catenin signaling and $G\alpha_s$-cAMP signaling. We identified a specific PKA phosphorylation site (Thr^{1548}) in the cytoplasmic domain of LRP6, phosphorylation of which "primed" the sequential phosphorylation of an adjacent site (Ser^{1544}) by GSK-3. Mutation of these phosphorylation sites inhibited the binding of LRP6 to $G\alpha_s$, disrupted the localization of $G\alpha_s$ at the plasma membrane, and reduced the amount of cAMP produced in response to PTH. Therefore, the PKA phosphorylation site within LRP6 is critical for the amplification of $G\alpha_s$ signaling.

Several lines of evidence indicate that activation of GPCRs also activates β-catenin signaling (32–37). A study demonstrated that free $G\beta\gamma$ subunits recruited GSK-3β to the plasma membrane to promote the phosphorylation of LRP6 at its PPPS/TP sites and subsequent β-catenin signaling (38), suggesting that free $G\beta\gamma$ is a critical component in GPCR-activated β-catenin signaling. We previously found that PTH induces the phosphorylation of LRP6 at its PPPS/TP sites and that PKA also regulates this phosphorylation event (37). Here, we suggest that the increased binding of $G\alpha_s\beta\gamma$ to PKA-phosphorylated LRP6 accelerates the activation of G proteins, which would result in the increased release of free $G\beta\gamma$. The enhanced recruitment of GSK-3β to the plasma membrane by free $G\beta\gamma$ and the subsequent phosphorylation of LRP6 at the PPPS/TP sites could be one of the reasons for the involvement of PKA in GPCR-activated β-catenin signaling. The direct binding to axin of the free active form of $G\alpha_s$ is also a critical element for the activation of β-catenin signaling (35). Together, this suggests that LRP6 activates $G\alpha_s$-cAMP signaling and β-catenin signaling sequentially. LRP6 recruits $G\alpha_s\beta\gamma$ to the plasma membrane to accelerate the activation of $G\alpha_s$ and its dissociation from $G\beta\gamma$, and the free $G\alpha_s$ and $G\beta\gamma$ subunits promote the activation of β-catenin signaling through two different pathways.

LRP6 interacts with an inactive conformation of $G\alpha_s\beta\gamma$. In response to PTH, $G\alpha_s$, $G\beta_1$, and $G\gamma_2$ form aggregates with LRP6 in fractions of the same molecular mass in ultracentrifugation gradients. The interaction of LRP6 with $G\alpha_s\beta\gamma$ was blocked by AlF_4^-, suggesting that $G\alpha_s$ mediated the interaction between LRP6 and the heterotrimer and that LRP6 did not bind to the active form of $G\alpha_s$. In addition, both $G\alpha_s$ and $G\beta_1$ translocated from the plasma membrane to the cytosol in cells in which LRP6 was knocked down, providing further evidence to support the idea that the $G\alpha_s\beta\gamma$ heterotrimer, but not the free active form of $G\alpha_s$, was the target of LRP6. The enriched $G\alpha_s\beta\gamma$ heterotrimer on the cell membrane would provide sufficient amounts of the inactive form of $G\alpha_s$, leading to accelerated activation of $G\alpha_s$ and the subsequent production of cAMP in response to agonist. We found that the interactions between LRP5 or LRP6 and the $G\alpha_s$ complex were different. PTH stimulated the binding of $G\alpha_s$ to LRP6, but not LRP5, and PKA phosphorylated LRP6, but not LRP5, in response to PTH. Therefore, the basal interaction of $G\alpha_s$ with LRP5 or LRP6 was independent of phosphorylation status, and phosphorylation enhanced the binding of $G\alpha_s$ to LRP6.

$G\alpha_s$ translocated from the plasma membrane to the cytosol in LRP6-deficient cells and in osteoblasts in the trabecular bone tissue of LRP6 knockout mice. Moreover, mutation of LRP6 at its PKA phosphorylation site reduced the amount of $G\alpha_s$ localized to the plasma

membrane and increased the cytosolic localization of $G\alpha_s$. $G\alpha_s$ is an essential component of the cAMP production system on the plasma membrane. Thus, LRP6-mediated trafficking of $G\alpha_s$ to the plasma membrane could set up a functional GPCR-$G\alpha_s$-AC complex for the rapid production of cAMP. $G\alpha_s$ is bound to the plasma membrane through a combination of lipid modification and its association with the $G\beta\gamma$ subunits (48). Although a family of palmitoyl acyltransferases (PATs) has been identified (49), the mechanisms by which $G\alpha_s$ is palmitoylated are unclear. Loss of LRP6 might disrupt lipid modification of $G\alpha_s$ and indirectly affects its localization to the plasma membrane.

The central role of LRP6 in the $G\alpha_s$-associated production of cAMP in response to GPCR stimulation in mammalian cells has a number of implications. Regulation of the production of cAMP by LRP6 may represent a previously uncharacterized control point that modifies the effects of ligand binding by $G\alpha_s$-associated GPCRs on transcription and other cell functions. This mechanism could potentially integrate hormonal and other $G\alpha_s$-coupled GPCR signals with other extracellular signals. Modulation of cAMP production through agents that target intracellular AC activity is targeted clinically in the treatment of many different diseases (50, 51). Targeting of LRP6 by its agonists or antagonists to modulate $G\alpha_s$ activity could provide another potential therapeutic approach.

MATERIALS AND METHODS

cDNA constructs

The complementary DNA (cDNA) sequence encoding PTH1R was subcloned into the plasmid pCDNA1 (52), the cDNA sequence encoding $G\alpha_s$ was subcloned into pCMV5B, the $G\alpha_s$-GFP cDNA was subcloned into the plasmid pCDNA3 (53), whereas the cDNA encoding VSVG-tagged LRP6 was subcloned into the plasmid pCS2+(26). We purchased siRNAs specific for GFP (sc-45924), mouse LRP5 (sc-149050), human LRP5 (sc-43900), mouse LRP6 (sc-37234), and human LRP6 (sc-37233) from Santa Cruz Bio-technology Inc. We generated cDNAs encoding VSVG-tagged $LRP6^{mGSK3}$ and $LRP6^{mPKA}$ by mutagenesis of the codons encoding Ser^{1544} or Thr^{1548} to a codon encoding alanine. Sequences encoding the cytoplasmic domain of LRP5 (amino acid residues 192 to 566, LRP5C) and the cytoplasmic domain of LRP6 (amino acid residues 461 to 593, LRP6C) were fused with cDNA encoding GST in the pGEX-KG prokaryotic gene fusion vector (Pharmacia). The mutants GST-$LRP6C^{mGSK3}$ and GST-$LRP6C^{mPKA}$ were generated by primer-mediated polymerase chain reaction (PCR) mutagenesis and verified by DNA sequencing. Sequences encoding FLAG-tagged $G\alpha_s$ and HA-tagged $G\beta_1$ at their N termini were subcloned into the plasmids pCMV5B and pCDNA3, respectively. The sequence of the siRNA specific for human axin (5′-UGCCAAGAAGGCUGAGUCG-3′) was designed as described previously (54).

Detection of cAMP

The amount of cAMP produced by cells in response to PTH or other GPCR agonists was determined with a ^3H-labeled cAMP assay, as described previously (55, 56). Briefly, cells were plated into six wells and incubated with 25 mM Hepes and [^3H]adenine (2 μCi/ml) at 37°C for 2 hours. After the isotope was removed by washing, cells were stimulated for 20 to 30 min at 37°C with PTH or other GPCR agonists in the presence of 1 mM IBMX (3-isobutyl-1-methylxanthine) and 0.4 mM ascorbate. Forskolin (10 μM) was used as a positive control. To terminate stimulation, we aspirated the media, added 1 ml of 5% trichloroacetic acid to each well, and stored the plates at 4°C overnight to collect the extracts. Separation of [^3H]cAMP from [^3H]ATP (adenosine 5′-triphosphate) was performed by chromatography on Dowex and alumina columns, according to the method of Salomon *et al.* (57). The

amount of cAMP formed from ATP was calculated as follows: % conversion = [^{3}H]cAMP/([^{3}H]cAMP + [^{3}H]ATP) × 100 per 20 or 30 min.

Detection of the temporal dynamics of cAMP signaling in living cells

The binding of cAMP to Epac induces a conformational change that liberates the catalytic domain of Epac from intrasubunit allosteric inhibition (42). A chimeric protein (ICUE3) generated by fusing the N terminus of a truncated form of Epac to enhanced CFP (ECFP) and the C terminus of Epac to citrine, an improved version of yellow fluorescent protein (YFP), was produced as previously described (43). Sandwiching these conformationally responsive elements of Epac between a FRET pair (citrine and ECFP) enables cAMP production and degradation to be monitored by detecting changes in FRET. Therefore, changes in cAMP could be monitored in real time in single live cells. Experiments were performed as previously described (41). HEK 293 cells plated on glass-bottom petri dishes (MatTek Corporation) were washed twice with buffer containing Hanks' balanced salt solution (HBSS) and placed on a Zeiss Axiovert 200M inverted microscope with a cooled charge-coupled device camera (MicroMAX BFT512, Roper Scientific). Cells were maintained in HBSS-containing buffer in the dark with the addition of PTH, isoproterenol, or forskolin as indicated in the figure legends. Cells were imaged with METAFLUOR 6.2 software (Universal Imaging) as the ratio between emission at 535 nm with a 535DF25 band-pass filter for citrine and emission at 475 nm with a 475DF40 bandpass filter for ECFP, upon excitation at 420 nm with a 420DF20 band-pass filter. Images were acquired every 30 s with an exposure time of 100 to 500 ms, which resulted in negligible photobleaching over a 30-min observation time. Fluorescent images were corrected for background by subtracting the autofluorescence intensities of untransfected cells (or the background with no cells) from the emission intensities of fluorescent cells that contained reporter constructs. The ratios of cyan-to-yellow emissions were then calculated at different time points and normalized by dividing all of the ratios by the emission ratio just before stimulation, thereby setting the basal emission ratio to 1. Citrine was photobleached at the end of the experiment by intense illumination with a 525DF40 filter. The fluorescence intensities of ECFP before (F_{da}) and after (F_d) citrine photobleaching and the equation $E = 1 - (F_{da}/F_d)$ were used to calculate the FRET efficiency.

Cell culture, transfections, coimmunoprecipitations, and Western blotting analysis

HEK 293, UMR-106, C2C12, and MEF cells were maintained in Dulbecco's modified Eagle's medium (DMEM) with 10% fetal calf serum (FCS). Transfections were performed with Lipofectamine reagent (Invitrogen). Immunoprecipitations and Western blotting analysis of cell lysates were performed as described previously (37). Briefly, cells were lysed in immunoprecipitation buffer [50 mM tris-HCl (pH 7.5), 150 mM NaCl, 1% Triton X-100, and 0.5% sodium deoxycholate] containing protease inhibitors. The lysates were subjected to immunoprecipitation by incubation with the appropriate antibodies followed by absorption on protein G–Sepharose. The immunoprecipitates were separated by SDS–polyacrylamide gel electrophoresis (SDS-PAGE) and transferred onto a nitrocellulose membrane. Western blots were characterized with the SuperSignal West Femto Substrate system (Pierce, Thermo Fisher Scientific Inc.). Primary antibodies used for Western blotting analysis and immunoprecipitations included mouse antibody against the FLAG tag (M2, Sigma-Aldrich), rabbit antibody against VSVG (Covance), mouse antibody against the HA tag (16B12, Covance), rabbit antibody against PTH1R (PRB-640P, Covance), rabbit antibodies against CREB and phosphorylated CREB (pCREB) (both from Upstate), and rabbit antibody against $G\alpha_s$ and mouse antibody against $G\beta_1$ (both from Santa Cruz Biotechnology).

GST fusion protein expression, pull-down assays, and in vitro kinase assays

The GST-tagged cytoplasmic domains of LRP5 (amino acid residues 192 to 566) and LRP6 (residues 461 to 593) and its mutant fragments were expressed in BL21 (DE3) *Escherichia coli* cells. The GST fusion proteins were then purified, and pull-down assays were performed as outlined previously (58). In vitro kinase assays were performed by the addition of bead-bound GST fusion proteins to buffer that contained 50 mM tris-HCl (pH 7.5), 10 mM $MgCl_2$, and 200 mCi [γ-^{32}P]ATP, together with the catalytic subunits of PKA, GSK-3β, or both in a volume of 30 μl. Reaction mixtures were incubated at room temperature for 30 min before the samples were resolved by 10% SDS-PAGE. The amount of protein-associated radiolabel was determined by PhosphorImager analysis (Molecular Dynamics).

Immunofluorescence detection of the localization of $G\alpha_s$, $G\beta_1$, and PTH1R

Cells stably expressing GFP-$G\alpha_s$ (53), GFP-$G\beta_1$ (59), or CFP-PTH1R were fixed with 100% methanol, permeabilized with 0.5% Triton X-100, and blocked in 2% bovine serum albumin in tris-buffered saline (TBS) containing 0.1% Tween 20. Digital pictures were taken with an Olympus IX TRINOC camera under an Olympus IX70 Inverted Research Microscope with a 10× objective lens and Hoffman modulation contrast at room temperature and processed with MagnaFire SP imaging software (Optronics). The numbers of cells with membrane-bound fluorescent protein or cytosolic fluorescent protein were quantified. For each treatment, 100 cells in three different slides were analyzed. The ratios of the number of cells with membrane-bound fluorescent protein or cytosolic fluorescent protein to the total cell numbers were calculated and expressed as a mean percentage ± SD.

Isolation and culture of primary mouse osteoblasts

Primary osteoblasts were obtained through serial digestion of calvaria of newborn mice in collagenase type I (1.8 mg/ml; Worthington Biochemical Corp.), as described previously (60). Briefly, calvaria from micewere digested in 10 ml of digestion solution for 15 min at 37°C with constant agitation. The supernatant was collected and replaced with fresh collagenase, and the digestion was repeated an additional four times. Final digestion solutions containing the osteoblasts were collected and centrifuged at 500*g* for 10 min at room temperature, and the osteoblasts were cultured in α-minimal essential medium (α-MEM) containing 10% fetal bovine serum (FBS) and 1% penicillin and streptomycin at 37°C in a humidified incubator supplied with 5% CO_2.

Generation of conditional *lrp6* knockout mice and bone immunohistochemistry analysis

The genotype of transgenic mice was determined by PCR analysis of genomic DNA isolated from mouse tails. Mice with osteoblast-specific inactivation of *lrp6* (*lrp6* knockouts) were generated by crossing *OC-Cre* mice with mice homozygous for a floxed *lrp6* allele. All mice were given a standard chow diet and water. Procedures involving mice were approved by the Institutional Animal Care and Use Program of the Johns Hopkins University. The mice were killed, and femora were resected and fixed in 10% buffered formalin for 48 hours, decalcified in 10% EDTA (pH 7.0) for 20 days, and embedded in paraffin. Immunostaining was performed with a standard protocol, as described previously (61). Sections were incubated with a 1:50 dilution of antibody against $G\alpha_s$ (Santa Cruz Biotechnology Inc.) overnight at 4°C. A horseradish peroxidase (HRP)–streptavidin detection system (Dako) was used to detect immunoreactivity, followed by counterstaining with methyl green (Sigma-Aldrich).

Supplementary Material

Refer to Web version on PubMed Central for supplementary material.

Acknowledgments

We thank F. Hunter and D. Nadziejka for critical reading of the manuscript, E. Xu for the glucagon receptor plasmid, T. J. Gardella for the pcDNA1-PTH1R plasmid, M. M. Rasenick for the $G\alpha_s$-GFP plasmid, and G. W. Zamponi for the GFP-$G\beta_1$ plasmid. **Funding:** This work was supported by NIH grants DK083350 (to M.W.), AR053973 (to X.C.), AR053293 (to B.O.W.), and DK073368 (to J.Z.).

REFERENCES AND NOTES

1. Selbie LA, Hill SJ. G protein-coupled-receptor cross-talk: The fine-tuning of multiple receptor-signalling pathways. Trends Pharmacol. Sci. 1998; 19:87–93. [PubMed: 9584624]
2. Ostrom RS, Post SR, Insel PA. Stoichiometry and compartmentation in G protein-coupled receptor signaling: Implications for therapeutic interventions involving G_s. J. Pharmacol. Exp. Ther. 2000; 294:407–412. [PubMed: 10900212]
3. Lefkowitz RJ. Seven transmembrane receptors: Something old, something new. Acta Physiol. 2007; 190:9–19.
4. Jüppner H, Abou-Samra AB, Freeman M, Kong XF, Schipani E, Richards J, Kolakowski LF Jr. Hock J, Potts JT Jr. Kronenberg HM, Segre GV. A G protein–linked receptor for parathyroid hormone and parathyroid hormone–related peptide. Science. 1991; 254:1024–1026. [PubMed: 1658941]
5. Abou-Samra AB, Jüppner H, Force T, Freeman MW, Kong XF, Schipani E, Urena P, Richards J, Bonventre JV, Potts JT Jr. Kronenberg HM, Segre GV. Expression cloning of a common receptor for parathyroid hormone and parathyroid hormone-related peptide from rat osteoblast-like cells: A single receptor stimulates intracellular accumulation of both cAMP and inositol trisphosphates and increases intracellular free calcium. Proc. Natl. Acad. Sci. U.S.A. 1992; 89:2732–2736. [PubMed: 1313566]
6. Gesty-Palmer D, Chen M, Reiter E, Ahn S, Nelson CD, Wang S, Eckhardt AE, Cowan CL, Spurney RF, Luttrell LM, Lefkowitz RJ. Distinct β-arrestin- and G protein-dependent pathways for parathyroid hormone receptor-stimulated ERK1/2 activation. J. Biol. Chem. 2006; 281:10856–10864. [PubMed: 16492667]
7. Rasmussen SG, Choi HJ, Rosenbaum DM, Kobilka TS, Thian FS, Edwards PC, Burghammer M, Ratnala VR, Sanishvili R, Fischetti RF, Schertler GF, Weis WI, Kobilka BK. Crystal structure of the human β2 adrenergic G-protein-coupled receptor. Nature. 2007; 450:383–387. [PubMed: 17952055]
8. Huber T, Menon S, Sakmar TP. Structural basis for ligand binding and specificity in adrenergic receptors: Implications for GPCR-targeted drug discovery. Biochemistry. 2008; 47:11013–11023. [PubMed: 18821775]
9. Sherwood NM, Krueckl SL, McRory JE. The origin and function of the pituitary adenylate cyclase-activating polypeptide (PACAP)/glucagon superfamily. Endocr. Rev. 2000; 21:619–670. [PubMed: 11133067]
10. Gelling RW, Du XQ, Dichmann DS, Romer J, Huang H, Cui L, Obici S, Tang B, Holst JJ, Fledelius C, Johansen PB, Rossetti L, Jelicks LA, Serup P, Nishimura E, Charron MJ. Lower blood glucose, hyperglucagonemia, and pancreatic α cell hyperplasia in glucagon receptor knockout mice. Proc. Natl. Acad. Sci. U.S.A. 2003; 100:1438–1443. [PubMed: 12552113]
11. Lolait SJ, O'Carroll AM, McBride OW, Konig M, Morel A, Brownstein MJ. Cloning and characterization of a vasopressin V2 receptor and possible link to nephrogenic diabetes insipidus. Nature. 1992; 357:336–339. [PubMed: 1534150]
12. Weinstein LS, Yu S, Ecelbarger CA. Variable imprinting of the heterotrimeric G protein $G_s\alpha$-subunit within different segments of the nephron. Am. J. Physiol. Renal Physiol. 2000; 278:F507–F514. [PubMed: 10751211]

13. Mountjoy KG, Robbins LS, Mortrud MT, Cone RD. The cloning of a family of genes that encode the melanocortin receptors. Science. 1992; 257:1248–1251. [PubMed: 1325670]
14. Getting SJ. Targeting melanocortin receptors as potential novel therapeutics. Pharmacol. Ther. 2006; 111:1–15. [PubMed: 16488018]
15. Leung PC, Wang J. The role of inositol lipid metabolism in the ovary. Biol. Reprod. 1989; 40:703–708. [PubMed: 2546614]
16. Ascoli M, Fanelli F, Segaloff DL. The lutropin/choriogonadotropin receptor, a 2002 perspective. Endocr. Rev. 2002; 23:141–174. [PubMed: 11943741]
17. Linder ME, Middleton P, Hepler JR, Taussig R, Gilman AG, Mumby SM. Lipid modifications of G proteins: α subunits are palmitoylated. Proc. Natl. Acad. Sci. U.S.A. 1993; 90:3675–3679. [PubMed: 8475115]
18. Wedegaertner PB, Bourne HR. Activation and depalmitoylation of $G_{s\alpha}$. Cell. 1994; 77:1063–1070. [PubMed: 7912657]
19. Kleuss C, Krause E. $G\alpha_s$ is palmitoylated at the N-terminal glycine. EMBO J. 2003; 22:826–832. [PubMed: 12574119]
20. Mumby SM, Casey PJ, Gilman AG, Gutowski S, Sternweis PC. G protein γ subunits contain a 20-carbon isoprenoid. Proc. Natl. Acad. Sci. U.S.A. 1990; 87:5873–5877. [PubMed: 2116011]
21. Lai RK, Perez-Sala D, Cañada FJ, Rando RR. The γ subunit of transducin is farnesylated. Proc. Natl. Acad. Sci. U.S.A. 1990; 87:7673–7677. [PubMed: 2217200]
22. Marrari Y, Crouthamel M, Irannejad R, Wedegaertner PB. Assembly and trafficking of heterotrimeric G proteins. Biochemistry. 2007; 46:7665–7677. [PubMed: 17559193]
23. He X, Semenov M, Tamai K, Zeng X. LDL receptor-related proteins 5 and 6 in Wnt/β-catenin signaling: Arrows point the way. Development. 2004; 131:1663–1677. [PubMed: 15084453]
24. Williams BO, Insogna KL. Where Wnts went: The exploding field of Lrp5 and Lrp6 signaling in bone. J. Bone Miner. Res. 2009; 24:171–178. [PubMed: 19072724]
25. Pinson KI, Brennan J, Monkley S, Avery BJ, Skarnes WC. An LDL-receptor-related protein mediates Wnt signalling in mice. Nature. 2000; 407:535–538. [PubMed: 11029008]
26. Tamai K, Semenov M, Kato Y, Spokony R, Liu C, Katsuyama Y, Hess F, Saint-Jeannet JP, He X. LDL-receptor-related proteins in Wnt signal transduction. Nature. 2000; 407:530–535. [PubMed: 11029007]
27. Mao B, Wu W, Li Y, Hoppe D, Stannek P, Glinka A, Niehrs C. LDL-receptor-related protein 6 is a receptor for Dickkopf proteins. Nature. 2001; 411:321–325. [PubMed: 11357136]
28. Bafico A, Liu G, Yaniv A, Gazit A, Aaronson SA. Novel mechanism of Wnt signalling inhibition mediated by Dickkopf-1 interaction with LRP6/Arrow. Nat. Cell Biol. 2001; 3:683–686. [PubMed: 11433302]
29. Sëmenov M, Tamai K, He X. SOST is a ligand for LRP5/LRP6 and a Wnt signaling inhibitor. J. Biol. Chem. 2005; 280:26770–26775. [PubMed: 15908424]
30. Ellies DL, Viviano B, McCarthy J, Rey JP, Itasaki N, Saunders S, Krumlauf R. Bone density ligand, Sclerostin, directly interacts with LRP5 but not $LRP5^{G171V}$ to modulate Wnt activity. J. Bone Miner. Res. 2006; 21:1738–1749. [PubMed: 17002572]
31. Li X, Zhang Y, Kang H, Liu W, Liu P, Zhang J, Harris SE, Wu D. Sclerostin binds to LRP5/6 and antagonizes canonical Wnt signaling. J. Biol. Chem. 2005; 280:19883–19887. [PubMed: 15778503]
32. Fujino H, Srinivasan D, Regan JW. Cellular conditioning and activation of β-catenin signaling by the FPB prostanoid receptor. J. Biol. Chem. 2002; 277:48786–48795. [PubMed: 12368277]
33. Farías GG, Godoy JA, Hernández F, Avila J, Fisher A, Inestrosa NC. M1 muscarinic receptor activation protects neurons from β-amyloid toxicity. A role for Wnt signaling pathway. Neurobiol. Dis. 2004; 17:337–348. [PubMed: 15474371]
34. Yang M, Zhong WW, Srivastava N, Slavin A, Yang J, Hoey T, An S. G protein-coupled lysophosphatidic acid receptors stimulate proliferation of colon cancer cells through the β-catenin pathway. Proc. Natl. Acad. Sci. U.S.A. 2005; 102:6027–6032. [PubMed: 15837931]

35. Castellone MD, Teramoto H, Williams BO, Druey KM, Gutkind JS. Prostaglandin E2 promotes colon cancer cell growth through a G_s-axin–β-catenin signaling axis. Science. 2005; 310:1504–1510. [PubMed: 16293724]
36. Gardner S, Maudsley S, Millar RP, Pawson AJ. Nuclear stabilization of β-catenin and inactivation of glycogen synthase kinase-3β by gonadotropin-releasing hormone: Targeting Wnt signaling in the pituitary gonadotrope. Mol. Endocrinol. 2007; 21:3028–3038. [PubMed: 17717075]
37. Wan M, Yang C, Li J, Wu X, Yuan H, Ma H, He X, Nie S, Chang C, Cao X. Parathyroid hormone signaling through low-density lipoprotein-related protein 6. Genes Dev. 2008; 22:2968–2979. [PubMed: 18981475]
38. Jernigan KK, Cselenyi CS, Thorne CA, Hanson AJ, Tahinci E, Hajicek N, Oldham WM, Lee LA, Hamm HE, Hepler JR, Kozasa T, Linder ME, Lee E. Gβγ activates GSK3 to promote LRP6-mediated β-catenin transcriptional activity. Sci. Signal. 2010; 3:ra37. [PubMed: 20460648]
39. Potts JT Jr. Murray TM, Peacock M, Niall HD, Tregear GW, Keutmann HT, Powell D, Deftos LJ. Parathyroid hormone: Sequence, synthesis, immunoassay studies. Am. J. Med. 1971; 50:639–649. [PubMed: 5575546]
40. Zylstra CR, Wan C, VanKoevering KK, Sanders AK, Lindvall C, Clemens TL, Williams BO. Gene targeting approaches in mice: Assessing the roles of LRP5 and LRP6 in osteoblasts. J. Musculoskelet. Neuronal Interact. 2008; 8:291–293. [PubMed: 19147944]
41. DiPilato LM, Cheng X, Zhang J. Fluorescent indicators of cAMP and Epac activation reveal differential dynamics of cAMP signaling within discrete subcellular compartments. Proc. Natl. Acad. Sci. U.S.A. 2004; 101:16513–16518. [PubMed: 15545605]
42. Violin JD, DiPilato LM, Yildirim N, Elston TC, Zhang J, Lefkowitz RJ. β2-Adrenergic receptor signaling and desensitization elucidated by quantitative modeling of real time cAMP dynamics. J. Biol. Chem. 2008; 283:2949–2961. [PubMed: 18045878]
43. DiPilato LM, Zhang J. The role of membrane microdomains in shaping β2-adrenergic receptor-mediated cAMP dynamics. Mol. Biosyst. 2009; 5:832–837. [PubMed: 19603118]
44. Seamon KB, Padgett W, Daly JW. Forskolin: Unique diterpene activator of adenylate cyclase in membranes and in intact cells. Proc. Natl. Acad. Sci. U.S.A. 1981; 78:3363–3367. [PubMed: 6267587]
45. Bilic J, Huang YL, Davidson G, Zimmermann T, Cruciat CM, Bienz M, Niehrs C. Wnt induces LRP6 signalosomes and promotes Dishevelled-dependent LRP6 phosphorylation. Science. 2007; 316:1619–1622. [PubMed: 17569865]
46. Pan W, Choi SC, Wang H, Qin Y, Volpicelli-Daley L, Swan L, Lucast L, Khoo C, Zhang X, Li L, Abrams CS, Sokol SY, Wu D. Wnt3a-mediated formation of phosphatidylinositol 4,5-bisphosphate regulates LRP6 phosphorylation. Science. 2008; 321:1350–1353. [PubMed: 18772438]
47. Fiol CJ, Wang A, Roeske RW, Roach PJ. Ordered multisite protein phosphorylation. Analysis of glycogen synthase kinase 3 action using model peptide substrates. J. Biol. Chem. 1990; 265:6061–6065. [PubMed: 2156841]
48. Resh MD. Palmitoylation of ligands, receptors, and intracellular signaling molecules. Sci. STKE. 2006; 2006:re14. [PubMed: 17077383]
49. Tsutsumi R, Fukata Y, Fukata M. Discovery of protein-palmitoylating enzymes. Pflugers Arch. 2008; 456:1199–1206. [PubMed: 18231805]
50. Pierre S, Eschenhagen T, Geisslinger G, Scholich K. Capturing adenylyl cyclases as potential drug targets. Nat. Rev. Drug Discov. 2009; 8:321–335. [PubMed: 19337273]
51. Pavan B, Biondi C, Dalpiaz A. Adenylyl cyclases as innovative therapeutic goals. Drug Discov. Today. 2009; 14:982–991. [PubMed: 19638320]
52. Schipani E, Karga H, Karaplis AC, Potts JT Jr. Kronenberg HM, Segre GV, Abou-Samra AB, Jüppner H. Identical complementary deoxyribonucleic acids encode a human renal and bone parathyroid hormone (PTH)/PTH-related peptide receptor. Endocrinology. 1993; 132:2157–2165. [PubMed: 8386612]
53. Yu JZ, Rasenick MM. Real-time visualization of a fluorescent $G\alpha_s$: Dissociation of the activated G protein from plasma membrane. Mol. Pharmacol. 2002; 61:352–359. [PubMed: 11809860]

54. Kim SM, Choi EJ, Song KJ, Kim S, Seo E, Jho EH, Kee SH. Axin localizes to mitotic spindles and centrosomes in mitotic cells. Exp. Cell Res. 2009; 315:943–954. [PubMed: 19331826]
55. Gallo-Payet N, Payet MD. Excitation-secretion coupling: Involvement of potassium channels in ACTH-stimulated rat adrenocortical cells. J. Endocrinol. 1989; 120:409–421. [PubMed: 2538537]
56. Kilianova Z, Basora N, Kilian P, Payet MD, Gallo-Payet N. Human melanocortin receptor 2 expression and functionality: Effects of protein kinase A and protein kinase C on desensitization and internalization. Endocrinology. 2006; 147:2325–2337. [PubMed: 16497811]
57. Salomon Y, Londos C, Rodbell M. A highly sensitive adenylate cyclase assay. Anal. Biochem. 1974; 58:541–548. [PubMed: 4827395]
58. Wan M, Cao X, Wu Y, Bai S, Wu L, Shi X, Wang N, Cao X. Jab1 antagonizes TGF-β signaling by inducing Smad4 degradation. EMBO Rep. 2002; 3:171–176. [PubMed: 11818334]
59. Doering CJ, Kisilevsky AE, Feng ZP, Arnot MI, Peloquin J, Hamid J, Barr W, Nirdosh A, Simms B, Winkfein RJ, Zamponi GW. A single Gβ subunit locus controls cross-talk between protein kinase C and G protein regulation of N-type calcium channels. J. Biol. Chem. 2004; 279:29709–29717. [PubMed: 15105422]
60. Zhang F, Qiu T, Wu X, Wan C, Shi W, Wang Y, Chen JG, Wan M, Clemens TL, Cao X. Sustained BMP signaling in osteoblasts stimulates bone formation by promoting angiogenesis and osteoblast differentiation. J. Bone Miner. Res. 2009; 24:1224–1233. [PubMed: 19257813]
61. Tang Y, Wu X, Lei W, Pang L, Wan C, Shi Z, Zhao L, Nagy TR, Peng X, Hu J, Feng X, Van Hul W, Wan M, Cao X. TGF-β1-induced migration of bone mesenchymal stem cells couples bone resorption with formation. Nat. Med. 2009; 15:757–765. [PubMed: 19584867]

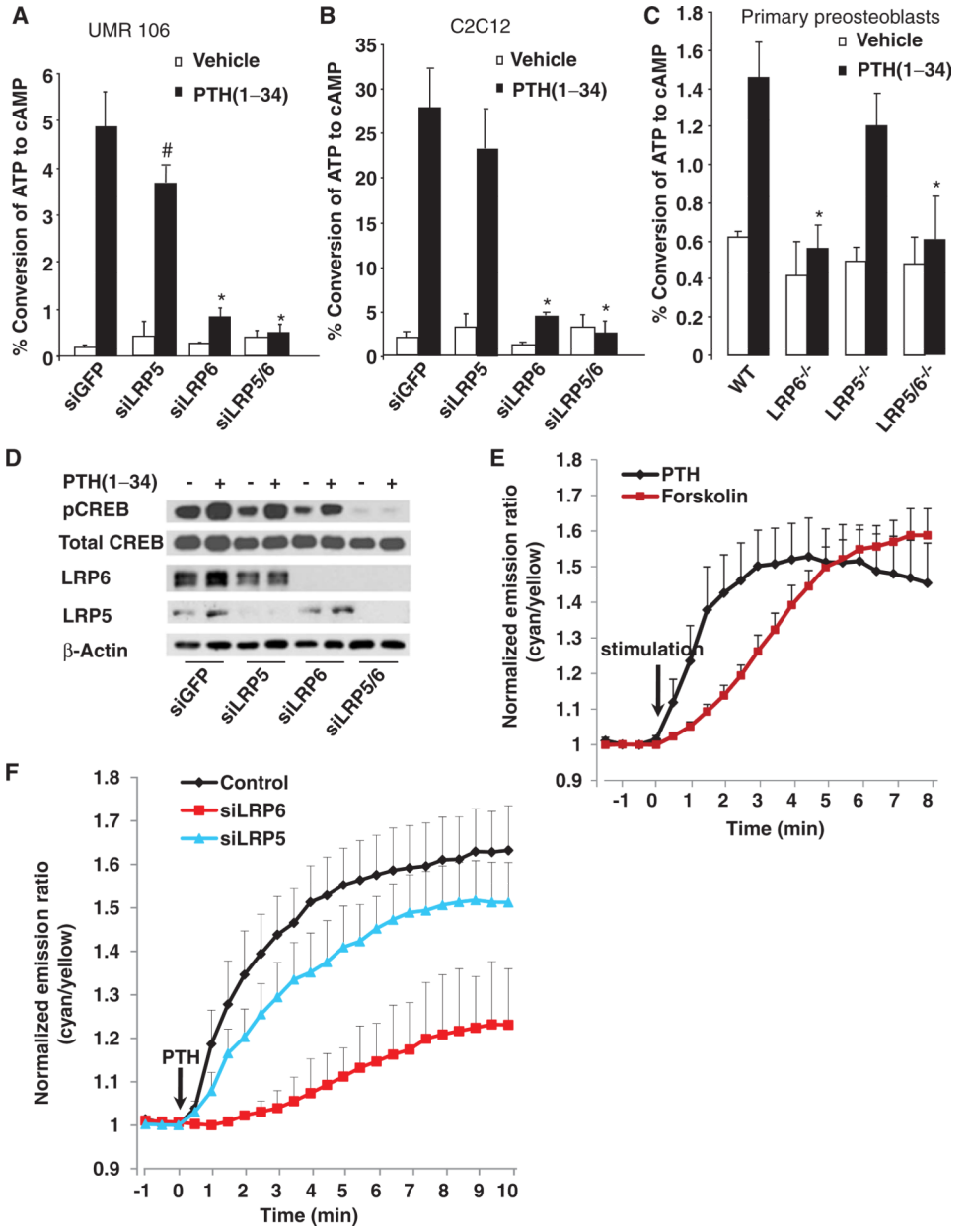

Fig. 1.

LRP6 is required for PTH-induced production of cAMP. (**A**) LRP6-specific siRNA inhibited PTH-induced cAMP accumulation in UMR-106 cells. Cells were transfected with siRNAs specific for GFP, LRP5, or LRP6 or with siRNAs against LRP5 and LRP6. Cells were treated with PTH(1–34) (50 nM) for 30 min and collected, and the amount of accumulated [^{3}H]cAMP was measured. Data are the means ± SD from three experiments. $^{\#}P < 0.05$, $*P < 0.001$ relative to the control cells treated with siRNA against GFP. (**B**) LRP6-specific siRNA inhibited PTH-induced cAMP accumulation in C2C12 cells. Cells were transfected, treated, and analyzed as described for (A). Data are the means ± SD from three experiments. $*P < 0.001$ relative to control cells treated with siRNA against GFP. (**C**) Accumulation of cAMP in response to PTH was abolished in LRP6-deficient primary calvarial preosteoblasts. Calvarial preosteo-blasts were isolated from *lrp6*-floxed or *lrp5*$^{-/-}$;*lrp6*-floxed newborn mice, infected with adenovirus expressing GFP or Cre, and treated with PTH(1–34) (50 nM)

for 30 min. Cells were collected, and the amount of accumulated [^{3}H]cAMP was measured. Data are the means ± SD from three experiments. *$P < 0.001$ relative to wild-type (WT) cells. (**D**) LRP6-specific siRNA attenuated the PTH-induced phosphorylation of CREB in UMR-106 cells. Cells were transfected and treated as described for (A). Cells were then collected and subjected to Western blotting analysis with antibodies against pCREB and total CREB. Data are representative of three experiments. (**E**) Representative emission ratio time courses (from six experiments) of ICUE3 stimulated with PTH(1–34) (50 nM) or forskolin (50 μM). (**F**) Representative emission ratio time courses (from six experiments) of ICUE3 stimulated with PTH(1–34) (50 nM) in control, LRP5 knockdown, or LRP6 knockdown cells.

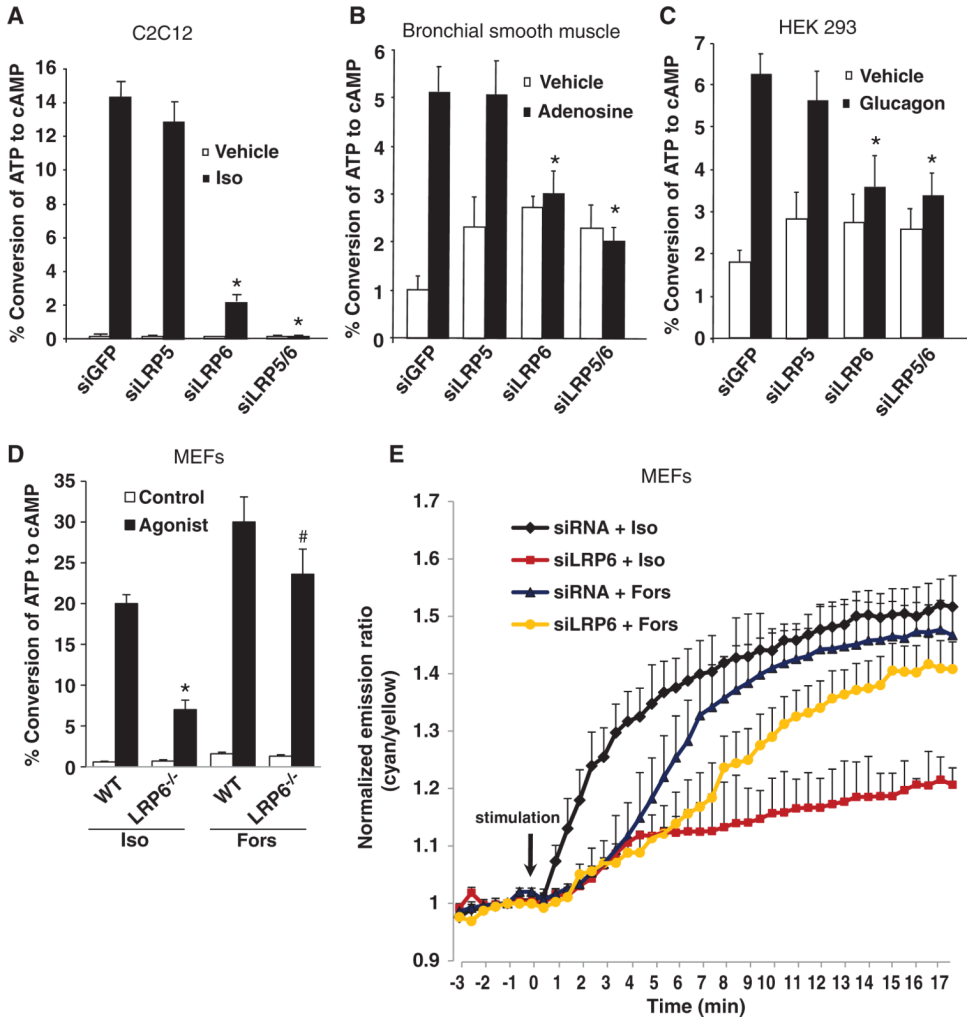

Fig. 2.

LRP6 is required for receptor-induced, $G\alpha_s$-coupled cAMP production. (**A**) LRP6-specific siRNA abolished isoproterenol-induced cAMP accumulation in C2C12 cells. Cells were trans fected with siRNAs against GFP, LRP5, or LRP6 or with siRNAs specific for LRP5 and LRP6. Cells were treated with isoproterenol (Iso, 10 nM) for 20 min, and the amount of accumulated [^{3}H]cAMP was measured. Data are the means ± SD from three experiments. *$P < 0.001$ relative to control cells treated with siRNA against GFP. (**B**) LRP6-specific siRNA abolished adenosine-induced cAMP accumulation in bronchial smooth muscle cells. Cells were transfected as described for (A) and treated with adenosine (10 nM) for 30 min, and the amount of accumulated [^{3}H]cAMP was measured. Data are the means ± SD from three experiments. *$P < 0.005$ relative to control cells treated with siRNA against GFP. (**C**) LRP6-specific siRNA abolished glucagon-induced cAMP accumulation in HEK 293 cells. Cells were transfected with plasmid encoding the glucagon receptor and with siRNAs specific for GFP, LRP5, or LRP6 or with siRNA against the common region of LRP5 and LRP6, treated with glucagon (50 nM) for 30 min, and the amount of accumulated [^{3}H]cAMP was measured. Data are the means ± SD from three experiments. *$P < 0.005$ relative to control cells treated with siRNA specific for GFP. (**D**) The accumulation of cAMP in LRP6-deficient MEFs in response to forskolin was less affected than that induced by isoproterenol. MEFs were isolated from *lrp6*-floxed or *lrp5*$^{-/-}$;*lrp6*-floxed newborn mice, infected with adenovirus expressing GFP or Cre, and treated with isoproterenol (Iso, 10 nM)

or forskolin (Fors, 50 μM) for 30 min. Cells were collected, and the amount of accumulated [^{3}H]cAMP was measured. Data are the means ± SD from three experiments. $^{\#}P < 0.05$, $*P < 0.001$ relative to WT. (E) Representative emission ratio time courses (from six experiments) of ICUE3 stimulated with isoproterenol (10 nM) or forskolin (50 μM) in control and LRP6 knockdown cells.

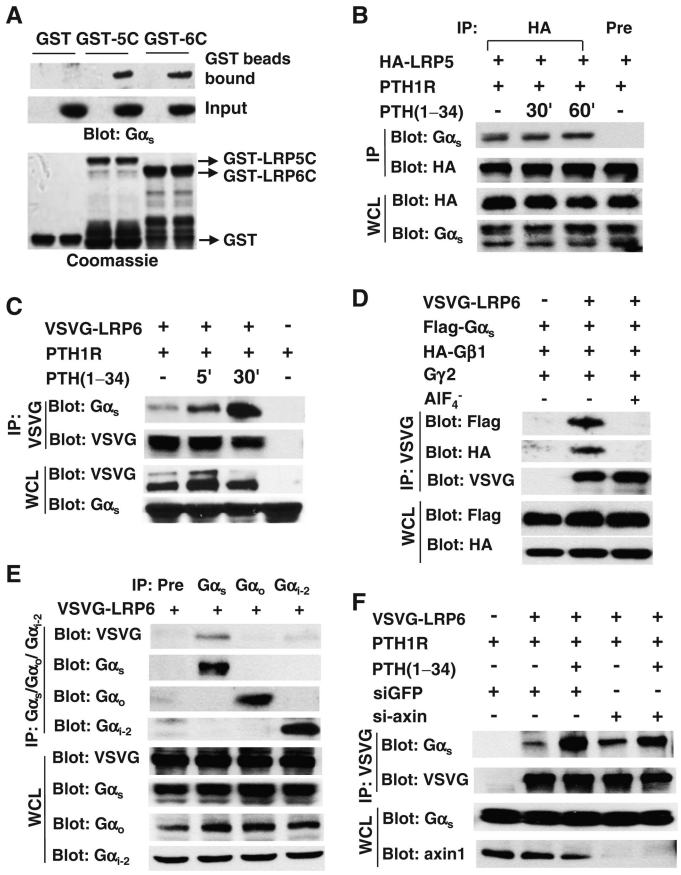

Fig. 3.

PTH promotes the association of LRP6 and $G\alpha_s$. (**A**) $G\alpha_s$ interacts with the cytoplasmic domain of LRP5 (LRP5C) and LRP6 (LRP6C). GST, GST-LRP5C, or GST-LRP6C was incubated with HEK 293 cell lysates. Bound $G\alpha_s$ was detected by Western blotting analysis with an antibody against $G\alpha_s$ (upper panel). $G\alpha_s$ in cell lysates was detected by Western blotting analysis with an antibody against $G\alpha_s$ (middle panel). The GST proteins were visualized by Coomassie brilliant blue staining (lower panel). (**B**) PTH does not affect the interaction between $G\alpha_s$ and LRP5. HEK 293 cells were transfected with plasmid encoding HA-tagged LRP5, deprived of serum for 14 hours to avoid protein phosphorylation by serum-derived hormones or growth factors, and treated with PTH(1–34) (50 nM). LRP5-associated $G\alpha_s$ was detected by Western blotting analysis of samples that were subjected to immunoprecipitation (IP) with an antibody against HA. Immunoprecipitation with a mouse preimmune antibody (Pre) was also performed as a negative control. WCL, whole-cell lysate. (**C**) PTH increases the extent of the interaction between $G\alpha_s$ and LRP6. HEK 293 cells were transfected with plasmid encoding VSVG-tagged LRP6, deprived of serum for 14 hours, and treated with PTH(1–34) (50 nM). LRP6-associated $G\alpha_s$ was detected by Western blotting analysis of samples immunoprecipitated with antibody against VSVG. (**D**) The interactions of LRP6 with $G\alpha_s$ and $G\beta_1$ are blocked by AlF_4^-. HEK 293 cells were transfected with plasmid encoding VSVG-tagged LRP6 together with plasmids encoding FLAG-tagged $G\alpha_s$, HA-tagged $G\beta_1$, and $G\gamma_2$ and were lysed in lysis buffer containing AlF_4^- (100 μM $AlCl_3$, 10 mM NaF). LRP6-associated $G\alpha_s$ and $G\beta\gamma$ were detected by Western blotting analysis of samples immunoprecipitated with antibody against VSVG. (**E**) LRP6 does not bind to $G\alpha_o$ or $G\alpha_{i2}$. HEK 293 cells were transfected with plasmid encoding VSVG-tagged LRP6. LRP6-associated $G\alpha_s$, $G\alpha_o$, and $G\alpha_{i2}$ were detected by Western

blotting analysis of samples immunoprecipitated with antibodies against $G\alpha_s$, $G\alpha_o$, and $G\alpha_{i2}$. Immunoprecipitation with a mouse preimmune antibody (Pre) was also performed as a negative control. (**F**) The PTH-induced interaction between $G\alpha_s$ and LRP6 was not affected by knockdown of axin. HEK 293 cells were transfected with scrambled control siRNA or siRNA specific for axin together with the indicated plasmids and treated with PTH(1–34) (50 nM). LRP6-associated $G\alpha_s$ was detected by Western blotting analysis of samples immunoprecipitated with antibody against VSVG.

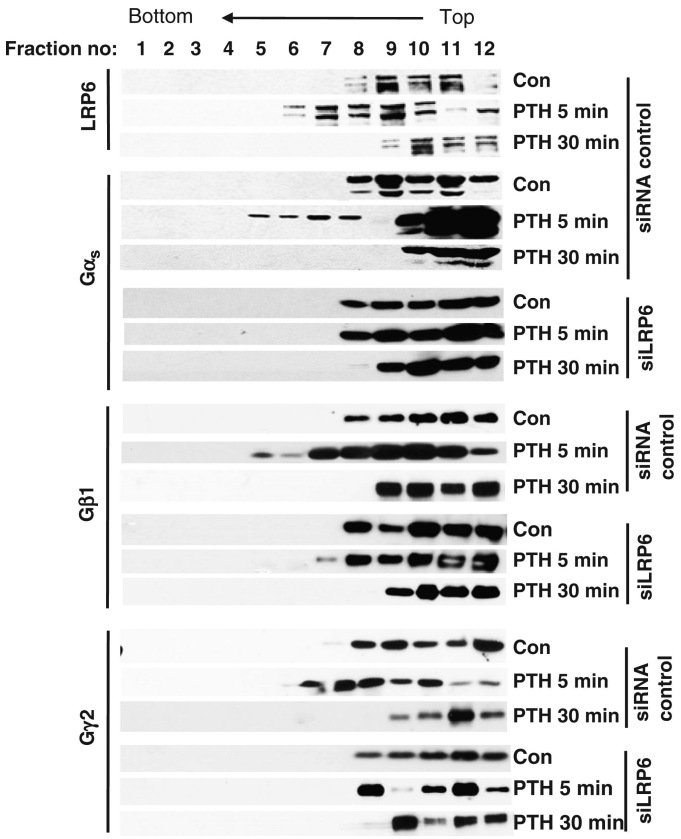

Fig. 4.

PTH induces LRP6 aggregation and $G\alpha_s\beta\gamma$ accumulation in UMR-106 cells, as analyzed by sucrose gradient sedimentation. UMR-106 cells were transfected with siRNAs specific for GFP or LRP6, and were treated with PTH(1–34) (50 nM) for the indicated time periods. Cell ly-sates were subjected to sucrose density-gradient ultracentrifugation, and fractions were analyzed by Western blotting with antibodies against LRP6, $G\alpha_s$, $G\beta_1$, and $G\gamma_2$. Data are representative of three experiments.

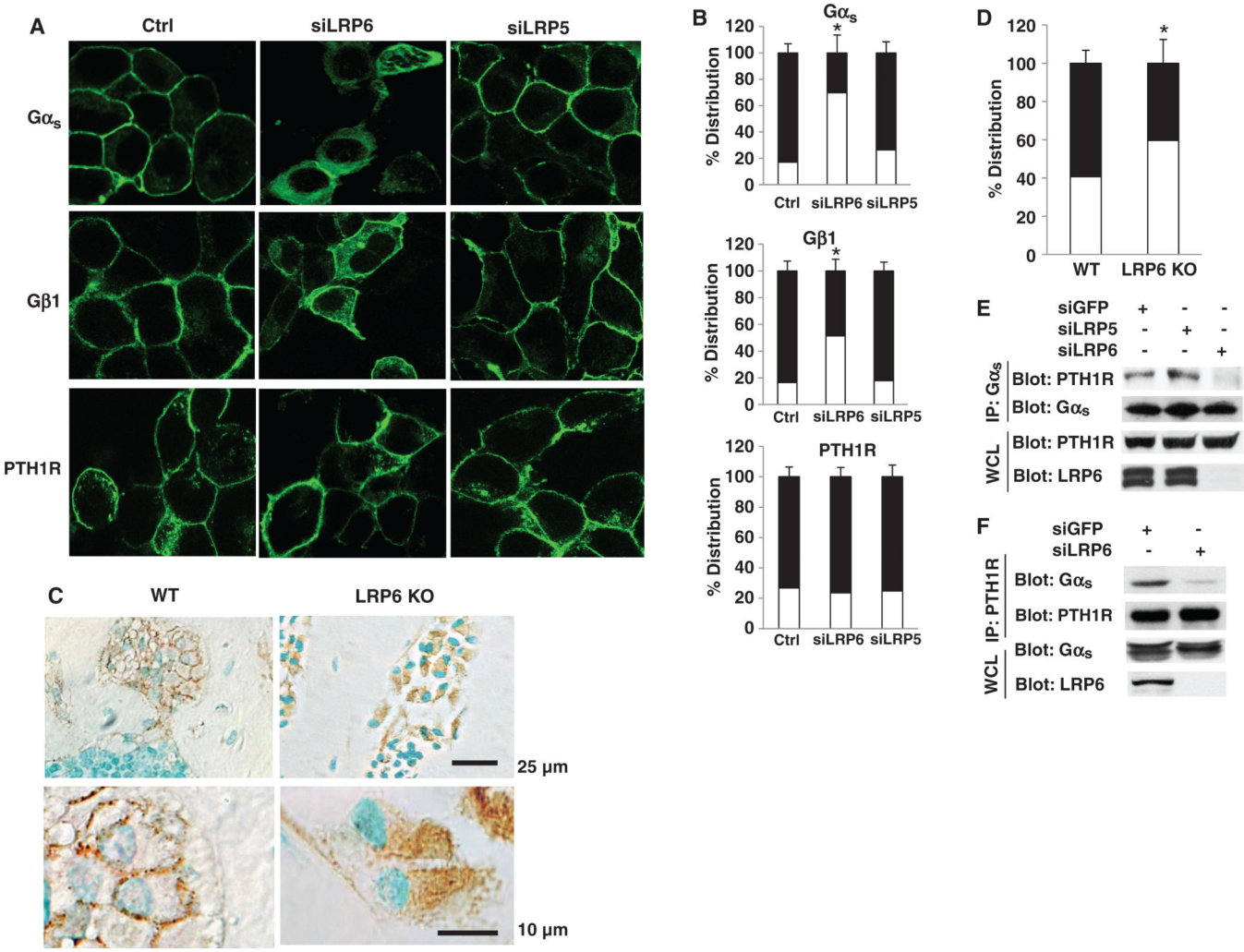

Fig. 5.

Knockdown of LRP6 impairs the targeting of $G\alpha_s$ to the plasma membrane. (**A**) Localization of $G\alpha_s$ and $G\beta_1$ to the plasma membrane is impaired by knockdown of LRP6. Stable HEK 293 cell lines expressing GFP-$G\alpha_s$, GFP-Gβ1, or CFP-PTH1R were transfected with siRNAs specific for LRP5 or LRP6 or with siRNA containing a random sequence (Ctrl). Green fluorescence was visualized by fluorescence microscopy. (**B**) Cells from (A) in which $G\alpha_s$, $G\beta_1$, or PTH1R was localized primarily at the plasma membrane or in the cytosol were quantified. For each treatment, 100 cells on three different slides were analyzed. The number of cells in which fluorescent protein was localized to either the plasma membrane (black bars) or the cytosol (white bars) divided by the total number of cells was calculated and expressed as a percentage ± SD. $*P < 0.05$ relative to siRNA control cells. (**C**) Localization of $G\alpha_s$ to the plasma membrane is impaired by deletion of LRP6 in osteoblasts from mouse femur. Immunohistochemical analysis of the amount of $G\alpha_s$ in sections of femurs from 2-month-old male *lrp6*-floxed (WT) and *lrp6*-floxed;*OC-Cre* (KO) mice. Photos are representative of tissue sections stained for $G\alpha_s$ and counterstained with methyl green. $G\alpha_s$-containing osteoblasts were stained brown. Three random high-power fields per specimen and a total of six specimens in each group were analyzed. The image shown is from one of these specimens. (**D**) Osteoblasts from (C) in which $G\alpha_s$ was localized to the plasma membrane or to the cytosol were counted in a blinded fashion from three random high-power fields per specimen in a 2-mm square, 1 mm distal to the lowest

point of the growth plate in the secondary spongiosa; a total of six specimens in each group were used. The osteoblasts in which $G\alpha_s$ was localized either to the plasma membrane (black bars) or to the cytosol (white bars) are presented as a percentage of the total number of osteoblasts. $*P < 0.05$ relative to WT samples. (**E** and **F**) The interaction between $G\alpha_s$ and PTH1R is attenuated by knockdown of LRP6. HEK 293 cells were transfected with siRNA specific for GFP or LRP6. Reciprocal immunoprecipitations were performed to identify the interaction between PTH1R and $G\alpha_s$. Data are representative of three experiments.

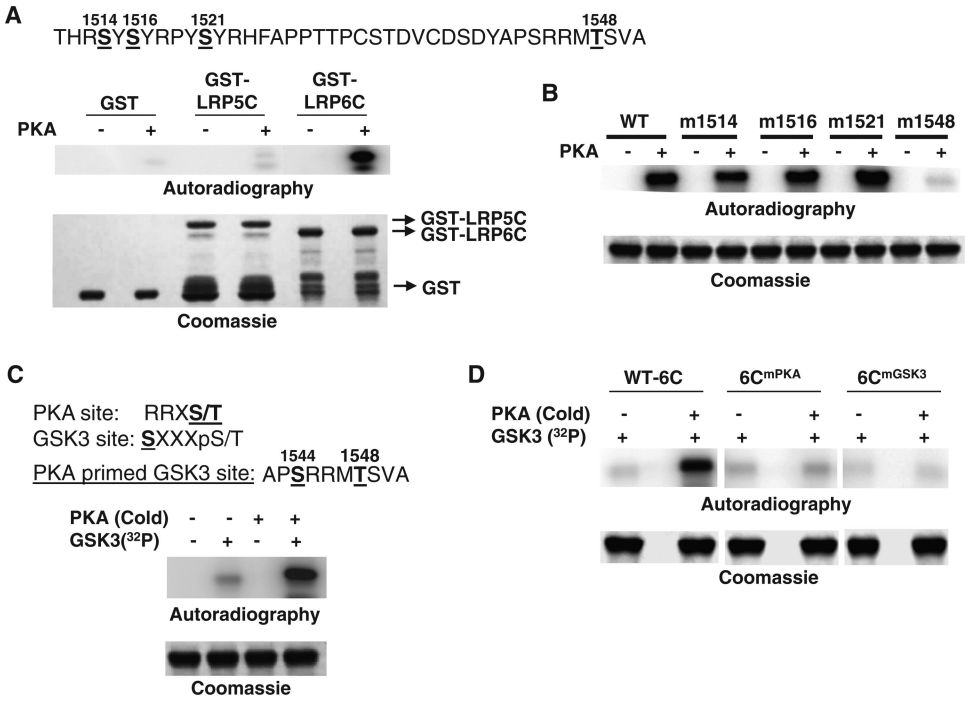

Fig. 6.

Phosphorylation of LRP6 by PKA enhances the binding of LRP6 to $G\alpha_s$. (**A**) PKA directly phosphorylates the intracellular domain of LRP6, as determined by in vitro kinase assay. The consensus PKA phosphorylation sites in the intracellular domain of LRP6 are shown at the top. GST, GST-LRP5C, and GST-LRP6C proteins were pulled down by glutathione beads. The bead-bound proteins were incubated with the recombinant catalytic subunit of PKA and [γ-^{32}P]ATP, and the protein-associated radiolabel was visualized by PhosphorImager analysis (Autoradiography). The GST proteins were analyzed by SDS-PAGE and visualized by Coomassie Brilliant Blue staining. Data are representative of three experiments. (**B**) Mutation of Thr^{1548} of LRP6 abolishes the phosphorylation of LRP6C by PKA. WT or various point-mutated GST-6C proteins were pulled down by glutathione beads. The bead-bound proteins were incubated with the catalytic subunit of PKA and [γ-^{32}P]ATP, and the protein-associated radiolabel was analyzed by SDS-PAGE and visualized by PhosphorImager analysis (Autoradiography). The GST proteins were visualized by Coomassie Brilliant Blue staining. Data are representative of three experiments. (**C**) Phosphorylation of LRP6C by PKA primes its phosphorylation by GSK-3. The consensus PKA and GSK-3 phosphorylation sites are shown at the top. GST-6C proteins were pulled down by glutathione beads. The bead-bound proteins were incubated with the catalytic subunit of PKA and cold ATP, washed, and then incubated with recombinant GSK-3 and [γ-^{32}P]ATP. The protein-associated radiolabel was analyzed by SDS-PAGE and visualized by PhosphorImager analysis (Autoradiography). The GST proteins were visualized by Coomassie brilliant blue staining. Data are representative of three experiments. (**D**) Mutation of the PKA or GSK-3 sites of LRP6 abolishes the sequential phosphorylation of LRP6C by PKA and GSK-3. WT (WT-6C) or the point-mutated GST-6C proteins, 6C^{mPKA} (Thr^{1548}→Ala) and 6C^{mGSK3} (Ser^{1544}→Ala), were pulled down by glutathione beads. The bead-bound proteins were then treated and analyzed as described for (A). The GST proteins were visualized by Coomassie Brilliant Blue staining. Data are representative of three experiments. Abbreviations for the amino acids are as follows: A, Ala; C, Cys; D, Asp; F, Phe; H, His; M, Met; P, Pro; R, Arg; S, Ser; T, Thr; V, Val; and Y, Tyr.

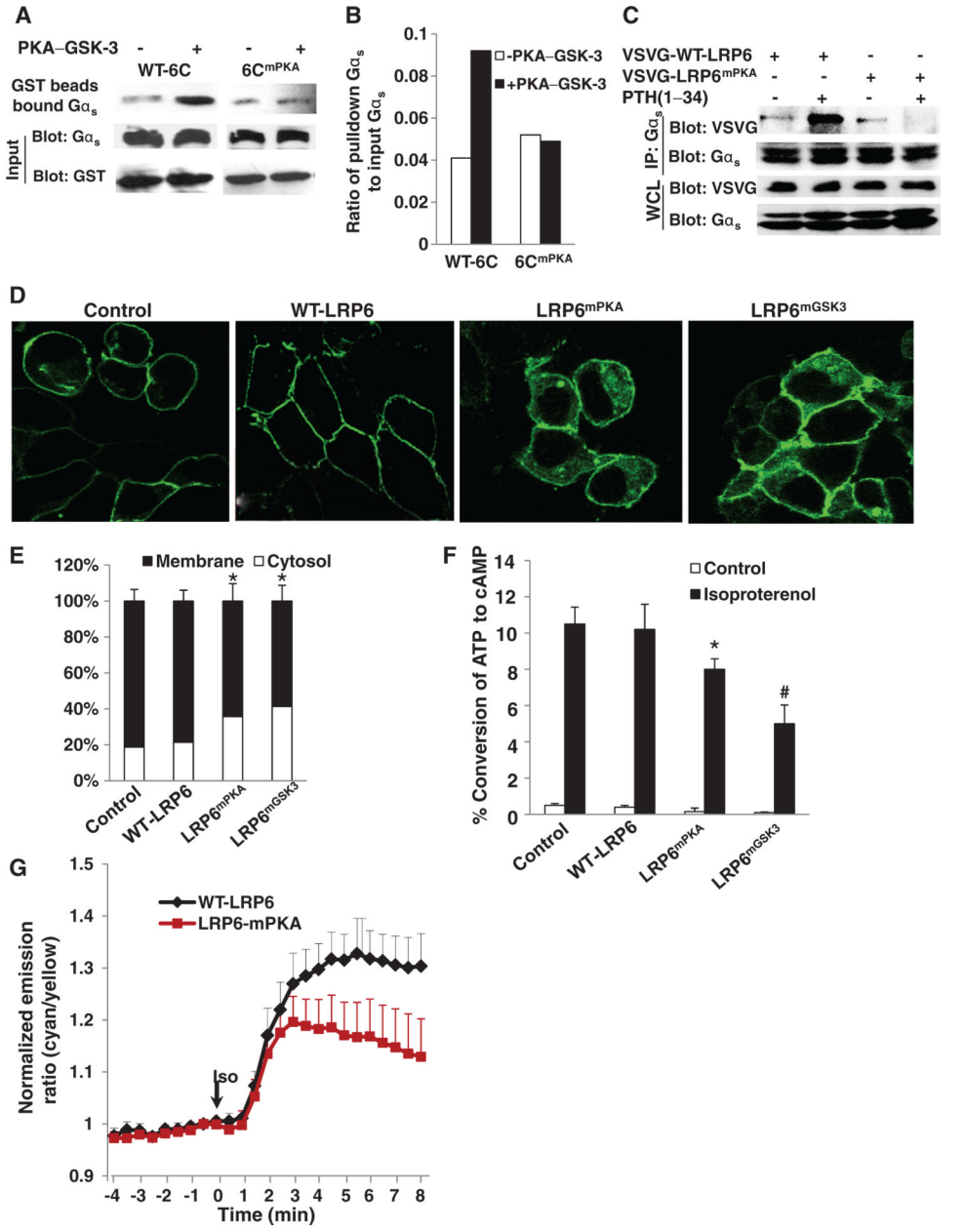

Fig. 7.

Phosphorylation of LRP6 by PKA and GSK-3 promotes the binding of $G\alpha_s$ to LRP6. (**A** and **B**) Mutation of the PKA site of LRP6 inhibits its binding to $G\alpha_s$ in vitro. GST-fused WT-6C or $6C^{mPKA}$ proteins were pulled down by glutathione beads. The bead-bound proteins were incubated with the catalytic subunit of PKA and ATP, washed, and then incubated with recombinant GSK-3 and ATP. The protein-associated beads were incubated with HEK 293 cell lysates. Bound $G\alpha_s$ was detected by Western blotting analysis with an antibody against $G\alpha_s$ (A, upper panel). The amounts of $G\alpha_s$ in the cell lysates and GST proteins were detected by Western blot analysis with an antibody against $G\alpha_s$ or GST (A, input panels). The intensities of the bands were quantitated by phosphorimaging and normalized to the density of the input amount of $G\alpha_s$ (B). (**C**) Mutation of the PKA site of LRP6 inhibits its binding to $G\alpha_s$ induced by PTH in cells. HEK 293 cells were transfected with plasmid

encoding VSVG-tagged WT-LRP6 or LRP6^{mPKA}. Cells were deprived of serum for 14 hours and treated with PTH(1–34) (50 nM). Gα_s-associated LRP6 was detected by Western blotting analysis of samples immunoprecipitated with antibody against Gα_s. Data are representative of three experiments. (**D**) Mutation of the PKA site of LRP6 impairs the localization of Gα_s to the plasma membrane. Stable HEK 293 cell lines expressing GFP-Gα_s were transfected with empty vector (Control) or plasmids encoding VSVG-tagged WT-LRP6, LRP6^{mPKA}, or LRP6^{mGSK3}. Green fluorescence was visualized by fluorescence microscopy. Data are representative of three experiments. (**E**) Cells from (D) in which localization of Gα_s was at the plasma membrane or in the cytosol were counted. For each treatment, 100 cells in three different slides were analyzed. The number of cells within which fluorescent protein was localized to the plasma membrane or the cytosol divided by the total number of cells was calculated and expressed as a percentage ± SD. *$P < 0.05$ relative to the empty vector control. (**F**) Accumulation of cAMP in MEFs in response to isoproterenol was reduced by mutation of the PKA or GSK-3 phosphorylation sites in LRP6. MEFs were isolated from E13.5 (embryonic day 13.5) mice and transfected with empty vector control or with plasmid encoding VSVG-tagged WT-LRP6, LRP6^{mPKA}, or LRP6^{mGSK3} and treated with isoproterenol (10 nM) for 20 min. Cells were collected and the amount of accumulated [^{3}H]cAMP was measured. *$P < 0.05$, $^{\#}P < 0.005$ relative to the cells containing empty vector control. (**G**) Representative emission ratio time courses (from eight experiments) of ICUE3 stimulated with isoproterenol (Iso, 10 nM) in cells containing WT LRP6 (WT-LRP6) or LRP6 with a mutation in the PKA phosphorylation site (LRP6-mPKA).

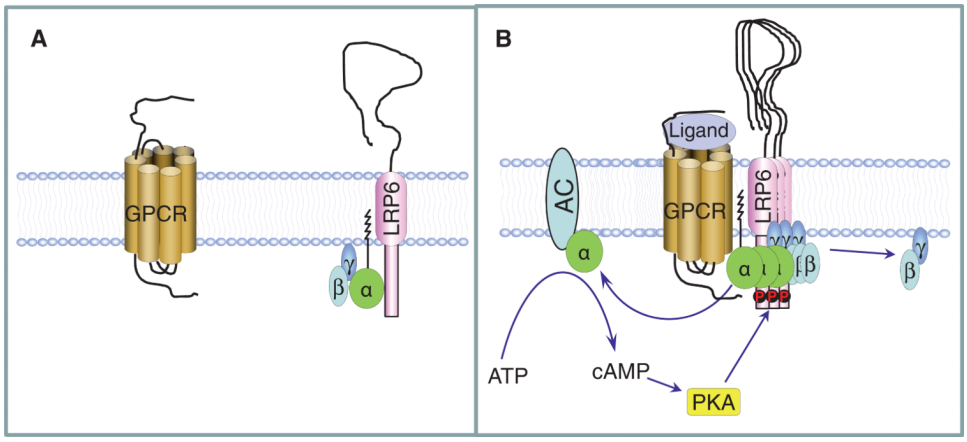

Fig. 8.

Schematic model of the involvement of LRP6 in $G\alpha_s$-coupled receptor signaling. (**A**) We propose that LRP6 binds to the inactive $G\alpha_s\beta\gamma$ heterotrimer on the plasma membrane in the absence of GPCR ligands. (**B**) Ligands induce the aggregation of LRP6 and cause the accumulation of $G\alpha_s\beta\gamma$ on the plasma member to set up a functional GPCR-$G\alpha_s$-AC complex for cAMP generation and PKA activation. Activated PKA, in turn, phosphorylates LRP6 and accelerates the binding of G protein complexes to LRP6 to enable enhanced production of cAMP.